http://dx.doi.org/10.5012/bkcs.2012.33.4.1363

Fabrication of Superhydrophobic Surface on Magnesium Substrate by Chemical Etching

Munhee Han, Seungcheol Go, and Yonghyun Ahn*

*Department of Chemistry, GRRC, Dankook University, Yongin 448-701, Korea. *E-mail: yhahn@dankook.ac.kr*
Received December 5, 2011, Accepted January 9, 2012

Key Words : Superhydrophobicity, Chemical etching, Nanospace, Lotus effect, Magnesium

Superhydrophobic surfaces are attractive because of their special wettability properties. In recent years, artificial superhydrophobic surfaces have been studied extensively because of the demand for self-cleaning materials.[1-6] The contact angle of water on a clean surface is a measure of its hydrophobicity. A water contact angle larger than 150° and a sliding angle less than 10° are the key characteristics of superhydrophobic surfaces. The wettability of a surface is controlled by its surface structure and chemical properties. In nature, many species demonstrate superhydrophobicity (e.g., lotus leaves and spiders).[7-11] The self-cleaning properties of lotus leaves are based on its papillae structure and wax coating. Coating a solid with a low surface energy material increases the water contact angle however; the contact angle of a flat surface generally does not exceed 120°. Therefore, it is necessary to alter the surface roughness to realize the high contact angle required for superhydrophobicity. A nano-to-micro-scale rough surface has been proven to be important for generating superhydrophobicity and the self-cleaning effect. Nano/micrometer binary structures create a rough surface that contains a large amount of air, which repels a water droplet. In general, the water contact angle is directly proportional to the amount of air trapped between the rough surface and water. To imitate the lotus leaf structure, many methods have been reported that alter a surface's roughness and structure, such as lithographic patterning,[12-14] chemical etching,[15,16] electrochemical deposition,[17,18] and the sol-gel method.[19,20] These surfaces have many applications, such as anti-fog, contamination prevention, and biocompatibility. The fabrications of superhydrophobic surfaces on magnesium,[21-23] copper,[24] zinc,[25] titanium,[26] and aluminum[27,28] have been achieved.

Magnesium is a key metal in the current industry because it has certain predominant physical properties, such as its light weight. Owing to its physical and mechanical properties, magnesium and its alloys are used in many industrial applications, such as airplanes, automobiles, ships, and cellular phones.

However, in practical applications, magnesium has a critical limitation, that is, low corrosion resistance. The fabrication of a superhydrophobic surface on magnesium would be a promising method to improve surface performance. The superhydrophobic surface on magnesium would reduce the full contact of the surface with water, which is one of the important factors required to overcome extremely low corrosion resistance.

Since the fabrication of a superhydrophobic surface on a magnesium alloy was first published in 2007,[29] a few methods have been reported on the superhydrophobic treatment of magnesium alloy surface.[22,23,30] Various methods have been proposed to achieve this, such as chemical and plasma etching, electrochemical deposition, and the sol-gel method.

In this paper, we describe a simple and efficient process for the fabrication of a superhydrophobic surface on magnesium alloy. This process combines chemical etching and treatment with stearic acid.

Experimental Section

Magnesium flakes (AZ31) with a size of 0.5 cm × 0.5 cm × 0.01 cm were cleaned ultrasonically in a solution of ethanol and distilled water for 5 min. The pieces were then immersed in a 5% HCl solution for 5 min and rinsed with distilled water. The total concentration of nickel sulfate hexahydrate [($NiSO_4 \cdot 6H_2O$), 1.31 g, 5 mmol] and hydrazine hydrate (0.62 g, 12.4 mmol) in 100 mL of H_2O was kept constant. Ethylenediamine dihydrochloride (2.19 g, 16.5 mmol) was then added to the reaction solution. The magnesium flakes were immersed in the solution and treated at 80 °C for 10 min and left to dry overnight at room temperature. After the magnesium flakes were dried, they were immersed in a solution of stearic acid and ethanol (1 g stearic acid in 100 mL EtOH) for 2 h and left to dry overnight at 50 °C.

Results and Discussion

It is well known that one way to make a surface superhydrophobic is to alter its surface roughness and then coat it with low-surface-energy materials. The maximum water contact angle of a flat surface is 120°, but the water contact angle on a hierarchical surface can reach ~170°.

With the addition of ethylenediamine·2HCl to a nickel electro-plating solution, Ni nanocones can be easily deposited on different metal surfaces.[17] Thus, ethylenediamine was initially chosen as a crystal modifier; however, results showed that ethylenediamine prohibited the formation of nickel particles. SEM imaging showed that when ethylenediamine

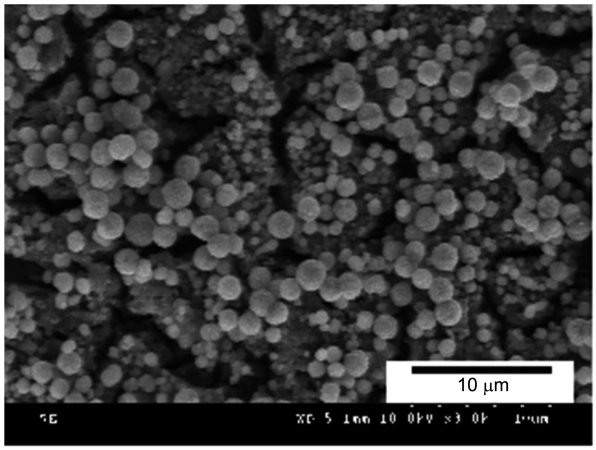

Figure 1. SEM image of Ni deposited on Mg surface.

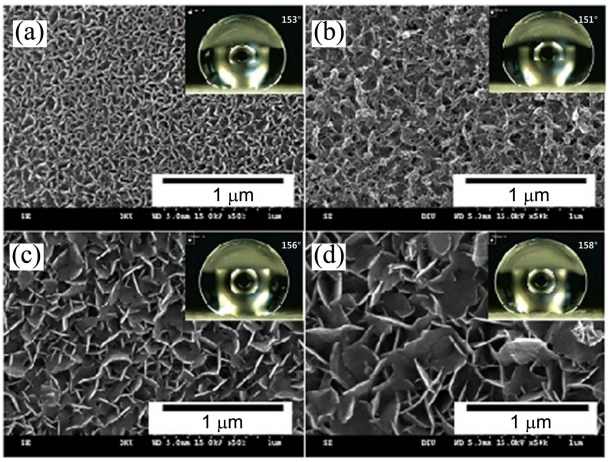

Figure 2. SEM images of magnesium surface etched with different dipping times. Inset shows a water droplet on the surface after it was treated with stearic acid. (a) 10 min, (b) 20 min, (c) 30 min, and (d) 40 min.

was introduced, the magnesium surface was etched despite the deposition of nickel particles. Figure 1 shows an SEM image of nickel-deposited on the Mg surface in the absence of ethylenediamine. The morphology of Ni is a ball structure. Figure 2 shows the magnesium surface after it was etched in the presence of ethylenediamine. The surface morphology varied with the dipping time. At the early stages, the etched Mg plate was a porous net structure. With an increase in the dipping time to 40 min, vertical plate-like structures were formed.

Long-chain *n*-alkanoic acids are environmentally friendly and can form self-assembled monolayers on metal surfaces. Stearic acid was used in this study because of its low surface energy.[31] After modification with stearic acid, the average contact angle was 152°. When a water droplet was dropped on an etched surface that was not treated with stearic acid, it spread on the surface. The chemically etched magnesium without modification with stearic acid showed the characteristics of superhydrophilicity; the contact angle was 43.1° (Figure 3).

The spaces in the hierarchical structure of the magnesium surface trap air, which in turn prevents the penetration of water into the space. The Cassie and Baxter equation[32,33] is used to understand the wettability of the interface between the space and a water droplet. The variable f is the fraction of the solid surface in contact with water, θ* is the normal contact angle of a rough surface, and θ is the contact angle of flat surface.

$$\cos \theta^* = f(\cos \theta + 1) - 1$$

Our fabricated surface exhibited a water contact angle of θ* = 152°. The water contact angle of an unetched magnesium surface coated with stearic acid is θ = 74.8°. The f value of the nano- and micro-structure was calculated to be 0.097. The low value of f indicated that the amount of solid surface in contact with water was reduced because of the increased roughness in the magnesium surface. The increased surface roughness corresponded with the increase in the contact angle. Thus, a large portion of air trapped in the surface was exposed, thereby preventing the penetration of water into the surface. This increased the water contact angle and enhanced the superhydrophobicity of the surface.

The surface morphology of the treated magnesium alloy was investigated using several analytical instruments. Figure 4 shows SEM image of a magnesium sample that was immersed for 4 h. The surface was composed of uniformly distributed pores with a diameter of 859.75 nm.

XPS was used to investigate the prepared thin film on the

Surface	Untreated magnesium plate	Chemically etched	Chemically etched and modified with stearic acid
Water contact angle(°)	CW ; 58.4°	CW ; 43.1°	CW ; 156.0°

Figure 3. Water contact angle on (a) untreated magnesium surface (b) chemically etched magnesium surface, and (c) chemically etched magnesium surface modified with stearic acid.

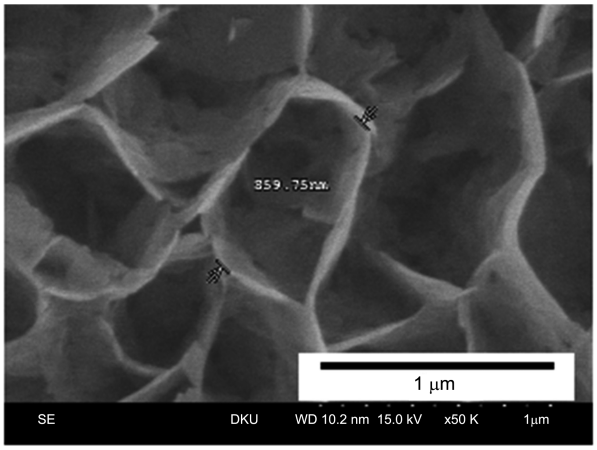

Figure 4. SEM image of magnesium surface etched for 4 h.

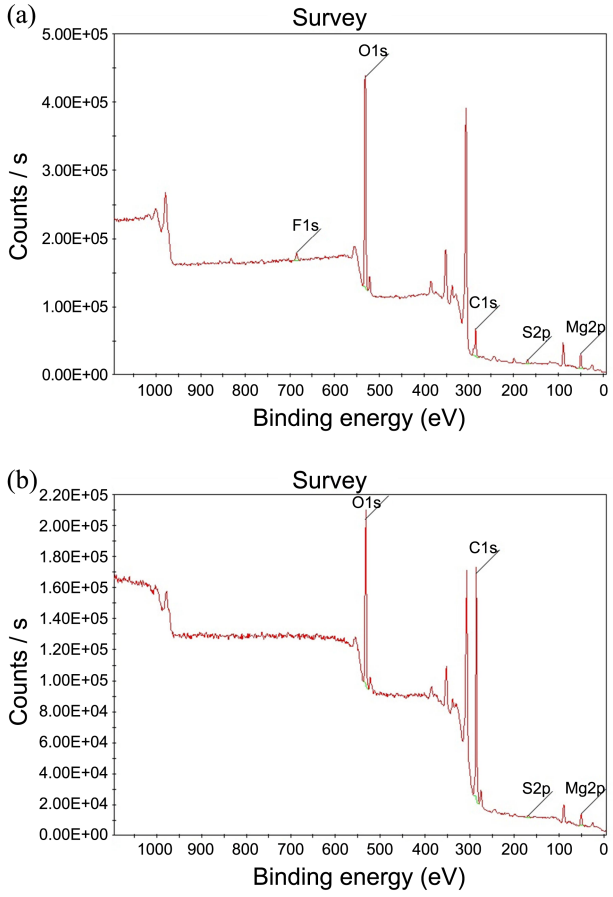

Figure 5. XPS spectrum of chemically etched magnesium surface (a) before and (b) after modification with stearic acid.

magnesium alloy surface. The element composition and contents of O, C, and Mg were evaluated. Figure 5 shows the XPS spectra of the unmodified surface (a) and the surface modified by stearic acid (b). O_{1s} and C_{1s} XPS signals were observed on the stearic acid modified surface of the magnesium alloy. The C content (C_{1s} = 284 eV) was remarkably higher for the modified surface. This verified that the surface was successfully coated with stearic acid and that the free energy of the surface was reduced.

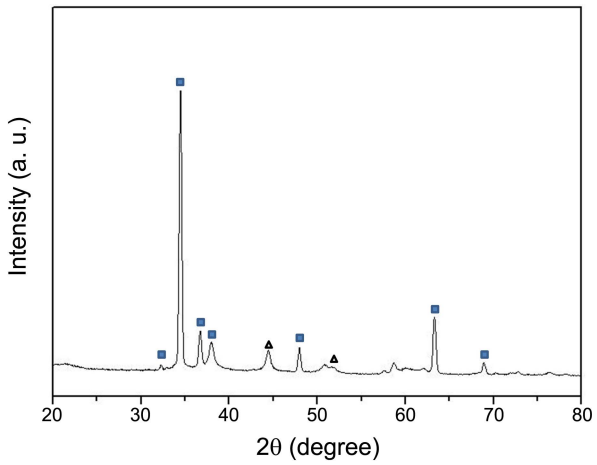

Figure 6. XRD pattern of chemically etched surface of magnesium alloy (□; Mg, △; Ni).

The chemical composition of the etched Mg surface before and after modification with stearic acid was studied using XRD spectroscopy. Figure 6 shows XRD patterns of the surface after it was chemically etched at 80 °C for 4 h in the presence of ethylenediamine. The characteristic peaks of magnesium were observed in the XRD spectrum, and it should be noted that the sample was detected to emit nickel signal. Diffraction peaks with an intensity as high as that of a pure Mg substrate were found, and it was inferred that nickel was deposited on some portion of the magnesium surface. The relatively low nickel peaks in the XRD spectrum were attributed to the reduction in the nickel substrate during immersion.

FT-IR analysis was used to confirm the presence of stearic acid on the coated surface of the Mg pieces.[34] Figure 7 shows the FT-IR spectrum of modified piece. Asymmetric and symmetric stretching of aliphatic CH_2 groups was observed at 2917 and 2857 cm^{-1}, respectively. A broad peak with maximum absorption at 3385 cm^{-1} corresponded to intermolecular hydrogen bonding, and the peak at 1432 cm^{-1} was ascribed to the vibration of the C-O group. Typically, the peak for the carboxyl group of stearic acid appears at

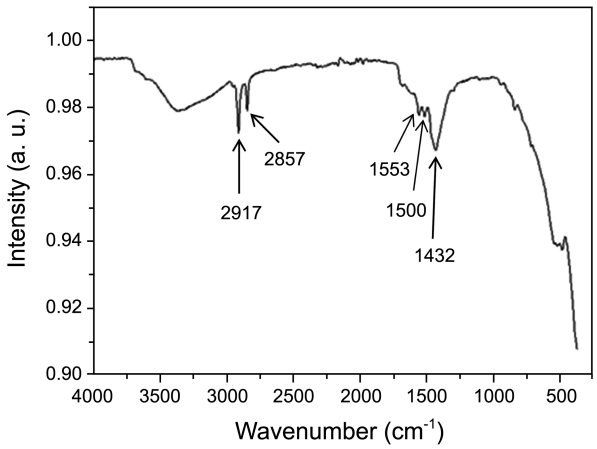

Figure 7. FT-IR spectrum of etched magnesium modified with stearic acid.

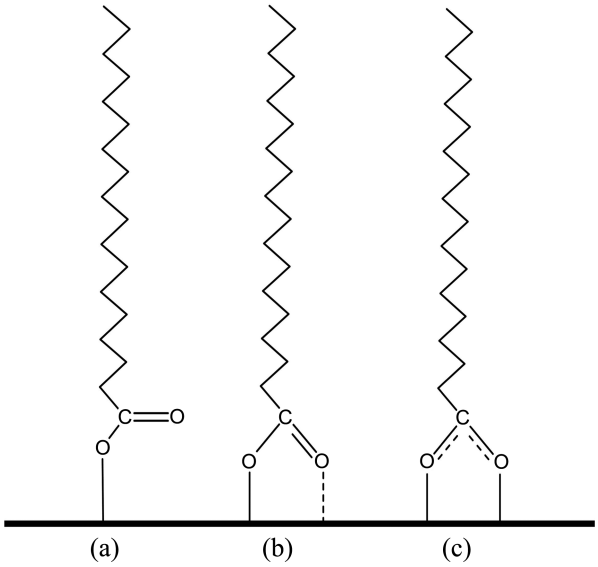

Figure 8. Stearic acid binding modes on metal oxide surfaces: monodentate (a), and bidentate [(b): asymmetric, (c): symmetric].

1710 cm^{-1}. However, the intensity of the peak decreased or shifted because of interactions between the carboxylic acid head group and the surface. The possible interactions were either a monodendate (with a peak at 1710 cm^{-1}) or a bidendate binding mode (caused by asymmetric and symmetric binding). The presence of a single peak at 1432 cm^{-1} indicated the symmetric binding mode of a carboxylate group. A doublet at 1553 and 1500 cm^{-1} indicated asymmetric stretching which is a type of bidentate binding. The binding modes were a combination of different interactions (Figure 8). These results revealed that stearic acid was bound to the magnesium surface via a bidentate interaction of carboxylate with two oxygen atoms and the disappearance of the C=O stretch band of the carboxyl group.

In conclusion, superhydrophobic surfaces were fabricated on magnesium flakes by a wet chemical etching method. As the immersion period increased, the chemical etching first created a nano-hierarchical structure on the magnesium surface, and subsequently changed the structure to a nano-vertical plate pattern. The nanostructured surface was coated with stearic acid, and it became superhydrophobic. Such a superhydrophobic surface can be used as an anticorrosion and self-cleaning surface.

Acknowledgments. This work was supported by the GRRC program of Gyeonggi province. [GRRC Dankook2011-B04, Development of advanced hard coating materials and processing methods].

References

1. Zhang, X.; Shi, F.; Niu, J.; Jiang, Y.; Wang, Z. *J. Mater. Chem.* **2008**, *18*, 621.
2. Roach, P.; Shirtcliffe, N. J.; Newton, M. I. *Soft Matter*. **2008**, *4*, 224.
3. Sun, T.; Feng, L.; Gao, X.; Jiang, L. *Acc. Chem. Res*. **2005**, *38*, 644.
4. Feng, L.; Li, S.; Li, Y.; Li, H.; Zhang, L.; Zhai, J.; Song, Y.; Liu, B.; Jiang, L.; Zhu, D. *Adv. Mater*. **2002**, *14*, 1857.
5. Park, Y.; Han, M.; Ahn, Y. *Bull. Kor. Chem. Soc*. **2011**, *32*, 1091.
6. Park, Y.; Ahn, Y. *Bull. Kor. Chem. Soc*. **2011**, *32*, 4063.
7. Barthlott, W.; Neinhuis, C. *Planta* **1997**, *202*, 1.
8. Neinhuis, C.; Barthlott, W. *Ann. Bot*. **1997**, *79*, 667.
9. Ball, P. *Nature* **1999**, *400*, 507.
10. Zhai, J.; Li, H. J.; Li, Y. S.; Li, S. H.; Jiang, L. *Physics* **2002**, *31*, 483.
11. Gao, X. F.; Jiang, L. *Nature* **2004**, *432*, 36.
12. Lee, S.; Lee, K.; Kim, J.; Lee, K.; Lee, S.; Hong, S. *Chem. Commun*. **2011**, *47*, 12005.
13. Lee, Y.; Park, S.; Kim, K.; Lee, J. *Adv. Mater*. **2007**, *19*, 2330.
14. Possato, A.; Zilio, S.; Fois, G.; Vendramin, D.; Mistura, G.; Belotti, M.; Chen, Y.; Natali, M. *Microelectron. Eng.* **2006**, *83*, 884.
15. Wang, Y. W.; Zhong, L.; Wang, J.; Jiang, Q.; Guo, X. *Appl. Surf. Sci*. **2010**, *256*, 3837.
16. Wang, H.; Dai, D.; Wu, X. *Appl. Surf. Sci*. **2008**, *254*, 5599.
17. Hang, T.; Li, M.; Fei, Q.; Mao, D. *Nanotechnology* **2008**, *19*, 35201.
18. Ghosh, P.; Yusop, M. Z.; Satoh, S.; Subramanian, M.; Hayashi, A.; Hayashi, Y.; Tanemura, M. *J. Am. Chem. Soc*. **2010**, *132*, 4034.
19. Lakshmi, R. V.; Bharathidasan, T.; Basu, B. *Appl. Surf. Sci*. **2011**, *257*, 10421.
20. Wang, S.; Liu, C.; Liu, G.; Zhang, M.; Li, J.; Wang, C. *Appl. Surf. Sci*. **2011**, *258*, 806.
21. Ishizaki, T.; Saito, N. *Langmuir* **2010**, *26*, 9749.
22. Liu, Y.; Li, L.; Lu, G.; Yu, S. *Sci. China Tech. Sci*. **2010**, *53*, 2972.
23. Chang, T.; Wang, J.; O, C.; Lee, S. *J. Mater. Proc. Tech.* **2003**, *140*, 588.
24. Guo, Z.; Fang, J.; Hao, J.; Liang, Y.; Liu, W. *ChemPhysChem* **2006**, *7*, 1674.
25. Hou, X.; Zhou, F.; Yu, B.; Liu, W. *Materials Sci. Engin. A* **2007**, *452*, 732.
26. Qu, M.; Zhang, B.; Song, S.; Chen, L.; Zhang, J.; Cao, X. *Adv. Funct. Mater*. **2007**, *17*, 593.
27. Jafari, R.; Farzaneh, M. *Appl. Phys. A* **2011**, *102*, 195.
28. Guo, Z.; Liu, W. *Appl. Phys. Lett*. **2007**, *90*, 223111.
29. Liang, J.; Guo, Z.; Fang, J.; Hao, J. *Chem. Lett*. **2007**, *36*, 416.
30. Yin, B.; Fang, L.; Hu, J.; Tang, A.; Wei, W.; He, J. *Appl. Surf. Sci*. **2010**, *257*, 1666.
31. Wang, Q.; Zhang, B.; Qu, M.; Zhang, J.; He, D. *Appl. Surf. Sci*. **2008**, *254*, 2009.
32. Wenzel, R. N. *Ind. Eng. Chem*. **1936**, *28*, 988.
33. Cassie, A. B. D.; Baxter, S. *Trans Faraday Soc*. **1994**, *40*, 546.
34. Lim, M.; Feng, K.; Chen, X.; Wu, N.; Raman, A.; Nightingale, J.; Gawalt, E. S.; Korakakis, D.; Hornak, L. A.; Timperman, A. T. *Langmuir* **2007**, *23*, 2444.